On the Performance of Ultra Wideband Radio in Stochastic Tapped Delay Line Model of the Ultra Wideband Channel

Kazi M. Ahmed, Mohammad Upal Mahfuz*, Rabindra Ghimire, and Mohammad E. R. Khan
Telecommunications Program, Asian Institute of Technology, PO Box: 4,
Khlong Luang, Pathumthani 12120, Thailand.
Email*: st100136@ait.ac.th

***Abstract*—This paper demonstrates the performance of Ultra Wideband (UWB) systems in the Stochastic Tapped Delay Line (STDL) model of the UWB channel with RAKE receiver. System models are based on Direct Sequence Code Division Multiple Access (DS-CDMA) principle. The system has been studied in presence of multiple user interference and Gaussian noise. During the analysis, various types of narrow, sub-nanosecond pulses with same power were used and extensive simulations were run in 3.1 to 10.6 GHz frequency band. The simulation results show that pulse shape has noticeable impact on the performance of the system. The performance of the pulse waveform based on third derivative of Gaussian pulse has proved to be better than other pulses that were used. With a thorough analytical approach, spectral behavior of higher order Gaussian pulses has been explained. Finally, it is concluded that the third derivative of Gaussian pulse is the most suitable pulse shape for fulfilling the FCC regulated power spectral diagram (PSD) has also been illustrated and in multi-user interference environment.**

***Index Terms*—Ultra wideband, channel model, pulse shape.**

I. Introduction

Ultra Wideband Impulse Radio (UWB-IR) is currently receiving a great deal of global attention because of its ability to provide higher data rate with low cost and relatively low power consumption. UWB radio communicates with baseband pulses of very short duration on the order of tenth of a nanosecond. According to the regulation of Federal Commission of Communications (FCC), a signal is defined as UWB signal if it has a -10 dB fractional bandwidth, F_{BW} greater than (or equal to) 0.20 or it occupies at least 500MHz of the spectrum [1] expressed as

$$F_{BW} = 2\frac{f_H - f_L}{f_H + f_L} \geq 0.20$$

where f_H and f_L correspond to the –10 dB bandwidths. FCC has also regulated the spectral shape and maximum power spectral density ($\approx$ -41.3 dBm/MHz) of the UWB radiation in order to limit the interference with other communication systems like UMTS or WLAN [2]. Although UWB impulse radio can be termed as 'Spread Spectrum' technique because of its extremely large operational bandwidth (7.5 GHz), the main difference is that conventional spread spectrum techniques utilize carriers for transmitting information whereas UWB radio transmits information without carrier. The waveforms that are used for UWB radio are very short in duration, causing their energy to be spread across the frequency spectrum. With UWB signals the dense multipath can be resolved, allowing a rake receiver for signal demodulation [3].

In order to analyze the potential of UWB systems, models describing the UWB propagation channel must be properly known. The channel models help analyze system performance and make design trades. In [4] the Statistical analysis of indoor radio propagation and the modified Poisson process or (Δ - K) model for path arrival of UWB system was presented. Examination of the Spread Spectrum (SS) principle with time hopping technique in the presence of wideband interference with AWGN channel has been considered [5]. The modified Poisson process or Δ-K model of the channel was used to study the UWB system for various M-PAM signals [6], but the channel model was not suitable for the UWB system because the frequency band used for measurement was in the range from 900 MHz to 1300 MHz. The effectiveness of multiuser detection for UWB using DS-CDMA was shown in [7]. A channel model based on measurements made in the indoor environment was presented in [8]. The model presented in [8] was formulated as a stochastic tapped delay line (STDL) model of the UWB indoor channel.

In this paper, to develop the UWB system model, DS-CDMA spreading approach, Stochastic Tapped Delay Line (STDL) model of the channel [8] and RAKE receiver in presence of multiple user interference are considered. The Bit Error Rate (BER) performance of DS-CDMA systems in UWB using STDL model and RAKE receiver with multiple user interference is shown. The effect of pulse shapes on channel characteristics has also been indicated. A thorough analytical explanation supporting the fact that third derivative of Gaussian pulse is the most suitable pulse shape for simultaneously fulfilling the FCC regulated power spectral density (PSD) has also been illustrated. Finally, on the basis of extensive simulations of BER performance and fulfillment of FCC power emission regulation, a conclusion has been drawn to choose the third derivative of Gaussian pulse as the best pulse shape for UWB radio communication.

The paper is organized as follows: Section II provides with a brief description of the concept of DS-CDMA based multi-user interference. The discussion is followed by Section III describing the complete STDL system model under investigation. Simulation environment and corresponding results have been explained in Section IV. Finally, Section V concludes the paper.

II. CONCEPT OF MULTI-USER INTERFERENCE

Multiple User Interference (MUI) is modeled as signals coming from other UWB users having the same basic signal characteristics as those of the user of interest, but using different spreading codes. Assuming a total of Nu users, the received signal $r(t)$ can be written as [9]

$$r(t) = s^{(1)}(t) \otimes h^{(1)}(t) + i(t) + n(t)$$

where $s^{(1)}(t)$ is the signal of interest at the output of the transmitting antenna, $h^{(1)}(t)$ represents the impulse response of the channel corresponding to the user of interest, $n(t)$ is the Gaussian noise and $i(t)$ is the interference coming from the other $(Nu-1)$ users. Here the interference, $i(t)$ can be defined as

$$i(t) = \sum_{n=2}^{Nu} s^{(n)}(t-\tau_n) \otimes h^{(n)}(t)$$

where $h^{(n)}(t)$ for $n = 2,3,.....Nu$ are the impulse responses of the channels corresponding to the $(Nu-1)$ interfering users and τ_n is the delay of the arrival time of the nth user from the user of interest i.e. $s^{(1)}(t)$ for which $\tau_1 = 0$. Assuming DS-CDMA as the used multiple access technique, $s^{(n)}(t)$ can be written as [9]

$$s^{(n)}(t) = \sum_{k=-\infty}^{+\infty} \sum_{j=1}^{Np} w_{d_k^{(n)}}(t - kT_d - jT_c)(c_p)^{(n)}$$

where $w(t)$ is the used pulse waveform, $(c_p)_j$ is the j-th chip of the Pseudo-random Noise (PN) code, generated by using bipolar PN sequences with values $\{+1,-1\}$, d_k is the k-th data bit chosen which, in Pulse Shape Mmodulation (PSM) case, also defines the pulse waveform to be transmitted, Np represents the number of pulses per data bit, Tc is the chip length and Td is the data bit length defined as $T_d = N_p T_c$. Each user experiences the channel with a different channel realization so that the channel impulse response

$$h^{(n)}(t) \neq h^{(m)}(t) \text{ where } n,m = 1,2,.....Nu, n \neq m$$

Each MUI user has the same power of the user of interest. Interfering users are considered either synchronous or asynchronous with the user of interest. The 'synchronous' condition refers to 'frame synchronization' where the receiver is synchronized with all other users and can receive all users' data at the same time instant. On the other hand, in the asynchronous case, the interfering signals arrive at the receiver with resolution of a time sample. The asynchronism is performed between every interfering user and the user of interest, and also among the interfering users.

III. SYSTEM MODEL

In this research study higher order derivatives of Gaussian and Rayleigh pulses have been used with STDL channel model. STDL channel model is a derivative of S-V model. STDL model has been chosen for channel representation because S-V channel has been very popular for indoor wireless channel modeling and many related studies have been based on this channel [9]. The time domain representations of some pulses are given in [10]. The overall block diagram of the proposed system is then shown in Figure 1.

A. *Sub-nanosecond mono-pulses*

The basic pulses used in simulation of this study are the nth order derivatives of Gaussian pulse expressed as

$$\Omega_G^n(t) = \frac{d^n}{dt^n}\left(\frac{A}{\sqrt{2\pi}\sigma} e^{-\left(\frac{t^2}{2\sigma^2}\right)}\right)$$

where the basic waveform of Gaussian pulse is given by

$$\Omega_{oG}(t) = \frac{A}{\sqrt{2\pi}\sigma} e^{-\left(\frac{t^2}{2\sigma^2}\right)}$$

In addition to above, the channel effects using Rayleigh pulse as expressed below are also compared.

$$\Omega_{oR}(t,\sigma) = \frac{t}{\sigma^2}\exp(-t^2/2\sigma^2)$$

Truncated *Sinc Pulse* and *Dual Gaussian Monopulse* were also used for simulation.

B. *Transmitter Section*

In the transmitter section Direct Spread CDMA spreading approach has been used. The equiprobable binary bit stream $\{b_j(i)\} \in \{1,-1\}$ is first multiplied by the spreading code, $c_j(k)$, named Walsh Hadamard Code of length 16. This DS-CDMA spreading is then followed by BPSK modulator where the spread output is BPSK modulated by a signature waveform, $\Omega_c(t)$. The modulated signal for the jth user is represented as [11]

$$x_j(t) = \sum_{i=-\infty}^{+\infty} \sum_{k=1}^{N} \Omega_c(t - iT_s - kT_c) c_j(k) b_j(i)$$

where, b_j(i) and $c_j(k)$ represent the ith information bit and the kth chip of the spreading code with length, N and chip duration, T_c respectively for the j-th user. T_s is the

symbol duration and $\Omega_c(t)$ is the chip pulse waveform. The radiated waveforms for Rayleigh Pulse and Third derivative of Gaussian pulse are shown in Figure 2(a) and 2(b).

C. Channel Model

The transmitted BPSK modulated signals, $x_j(t)$ are then passed through the STDL propagation channel model, which is based on measurements made in a typical office environment for UWB radio channel [8]. The model characterizes the shape of the power-delay profile (PDP) in terms of path gains, G_K and delays, τ_K of multipath components. The delay axis was adjusted in such a way that the delay bin of the first quasi Line of Sight (LOS) path began at time instant τ = 0. The path resolution of the considered system was $\Delta\tau = 2ns$. Before the signal is received by the receiver section, thermal noise, $n(t)$ and interference from narrow-band transmitters, $n_f(t)$ get added to it. The model represented the statistics of the path gains and its dependence on the delays.

The large-scale and the small-scale fading statistics were also distinguished. The Power Delay Profile (PDP) at one location and that averaged over all locations within the measurement area were referred to as 'Local PDP' and 'Small Scale Averaged PDP (SSA-PDP)' respectively. Large scale fading was investigated by considering the SSA-PDPs of different locations, i.e. after having removed partially the small scale statistics by spatially averaging the PDPs over the locations within one measurement area. The 'global' parameters, referring to large scale and small scale fading effect of the channel respectively, have been shown in Table 1.

For large scale fading, the SSA-PDP exhibits an exponentially decay function of excess delay. The power ratio, r and the decay constant, ε, which vary from location to location, were treated as stochastic variables. Since there were limited values of r and ε, they were modeled as Log-Normal variables [8] as shown in Table 1. The path loss (PL) was defined as a function of distance also as shown in Table 1 [8]. The total average energy gain, $\overline{G}_{tot}$ can be calculated by integrating the SSA-PDP of each place over all delay bins. The $\overline{G}_{tot}$ is also log-normally distributed about path loss (PL) and a standard deviation of 4.3 [8]. The average PDP is specified according to [8]

$$\overline{g}(\tau) = \frac{\overline{G}_{tot}}{1 + r\dfrac{1}{1 - e^{(-\Delta\tau/\varepsilon)}}} \left\{ \begin{array}{l} \delta(\tau - \tau_1) + \\ \sum_{k=2}^{N_{bins}} [re^{-((\tau_k - \tau_2)/\varepsilon)}]\delta(\tau - \tau_k) \end{array} \right\}$$

On the other hand, small-scale fading characterizes the changes in the received signal when the receiver position changes only by a small fraction of the distance between transmitter and receiver. This was derived by considering the deviations of all the local PDP from the respective SSA-PDP. The 'local' parameters, referring to small scale fading effect, have also been shown in Table 1. The local path gain values, G_k are the superposition of large and small scale statistics and are Gamma distributed random variables with mean, $\overline{G}_k$ and parameters, m_k. The values of m_k are independent truncated Gaussian random variables with parameters dependent on the delay, τ_k and mean, $\overline{G}_k = \overline{g}(\tau_k)$ [8].

The received signals are the sum of replicas of the transmitted signals. The received signal is, therefore, expressed as

$$r(t) = \sum_{i=1}^{N_{path}} (c_i x(t - \tau_i) + n(t) + n_f(t))$$

where, n(t) is zero mean AWGN and $n_f(t)$ is the interference signal.

D. Receiver Section

For the simulation of this study RAKE receiver with a maximum of 12 arms are used. First arm is locked to the first multipath component, m_1. Multipath component, m_2 arrive τ_1 time units later than m_1 and is captured by second tap and so on. The signals in the correlators are despread by Walsh Hadamard Code of length 16. All decision statistics are weighted by a weighting factor, α to form overall decision statistics. The signals are then integrated over the entire period the entire period. The integrated signal is then compared with the appropriate threshold value to receive the better estimate of the transmitted signal.

Table 1: Expressions of global and local parameters

Global Parameters:
$\text{Path Loss} = \begin{cases} 20.4.\log_{10}(d/d_0) & d \le 11m \\ -56 + 74.\log_{10}(d/d_0) & d > 11m \end{cases}$
Decay Constant $\varepsilon \sim L_N(16.1;1.27)$
Shadowing $\overline{G}_{tot} \sim L_N(-PL;4.3)$
Power Ratio $r \sim L_N(-4;3)$
Local Parameters:
Energy Gains $G_k \sim \Gamma(\overline{G}_k; m_k)$
$\text{m Values} \begin{cases} m_k \sim T_N(\mu_m(\tau_k); \sigma_m^2(\tau_k)) \\ \mu_m(\tau_k) = 3.5 - \dfrac{\tau_k}{73} \\ \sigma_m^2(\tau_k) = 1.84 - \dfrac{\tau_k}{160} \end{cases}$

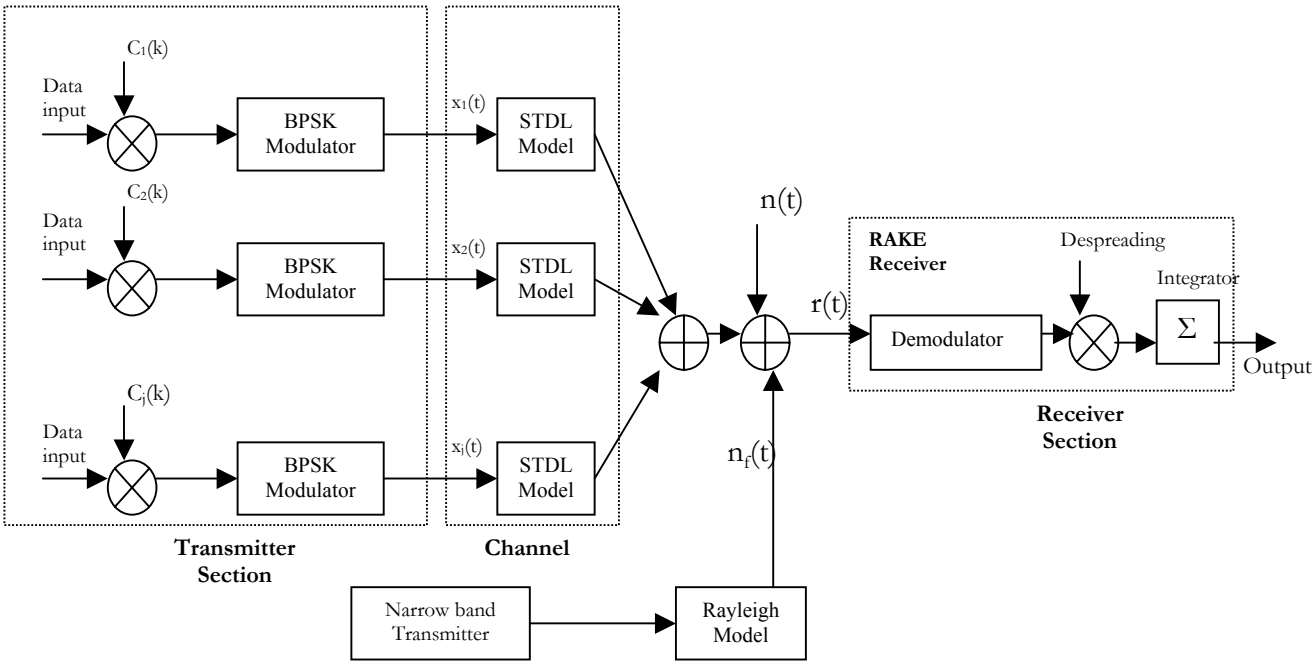

Figure 1: Block diagram of system model

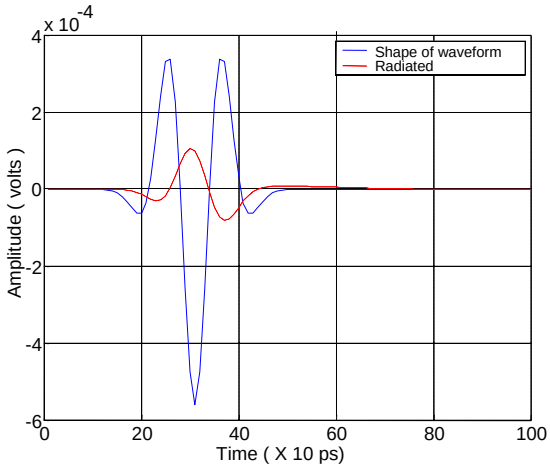

Fig. 2.b: Third Derivative of Gaussian Pulse

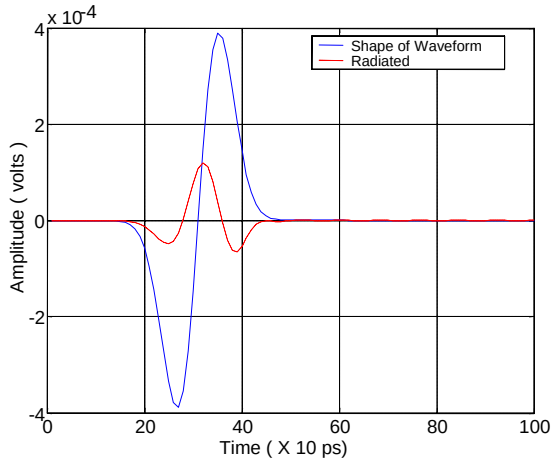

Fig 2.a: Rayleigh pulse

IV. Results

In this section, results based on the simulation of performance of an ultra wideband system using DS-CDMA multiple access technique, Stochastic Tapped Delay Line (STDL) channel model and RAKE receiver with individual cases of 8 and 12 Rake arms and various types of sub-nanosecond pulses as well as multiple user interference (MUI) have been presented. The chip rate is 320 Mchip/s with spreading length of 16 (Walsh Hadamard code). The arrival of multiple users is assumed to be Gaussian in nature and exist over the entire period. Performance of various sub-nanosecond pulses in STDL model has been discussed in the next sub-section which is followed by a discussion on results of system performance in the presence of multiple user interference.

A. The effect of pulse shapes on channel model

Figures 3.a and 3.b show the results of simulation for different pulse shapes with a number of Rake receiver taps equal to 8 and 12 at a distance of 5m with STDL model of the channel and in the presence of white Gaussian noise. For each case, synchronization and channel estimation are assumed to be perfect. The results show that the pulse shape has noticeable impact on the performance of the system. It has been found in simulation that the performance of third derivative of Gaussian pulse is better than any other pulses.

For the Bit Error Rate (BER) of 10^{-4}, using RAKE arms equal to 8 at a distance of 5m as shown in Figure 3.a, the third derivative of Gaussian pulse has 3.5 dB E_b/No gain over that value of Gaussian monopulse, whereas the fifth

derivative of Gaussian pulse has almost the same E_b/No ratio as that of Gaussian pulse. Similarly, for the BER of 10^{-4}, increasing the number of RAKE arms to 12, as shown in Figure 3.b at a distance of 5m the third derivative of Gaussian pulse has 2.9 dB E_b/No gain over that value of Gaussian monopulse, whereas the fifth derivative of Gaussian pulse needs 0.5 dB E_b/No more than what is required by the Gaussian pulse.

Pulse shape has noticeable impact because in the multipath environment there is more chance that the pulses will arrive with different delay, and the arrived components are out of phase with each other. In UWB systems, baseband pulses and BPSK modulation schemes have been used for simulation. If the arrived components are out of phase, in such case the resulting output of the receiver depends on pulse shape. A comparison between performances shown in Figure 3.a and Figure 3.b also indicates a performance improvement in multipath fading environment as a result of using an increased number of RAKE arms.

B. The effect of Multiuser Interference on System Performance

Figures 4.a, 4.b and 4.c show system performances in presence of multiple user interference at a distance of 5m. As shown in the above figures, it is found that degradation in the performance of third derivative of Gaussian pulse is less than the degradations of Rayleigh pulse and second derivative of Rayleigh pulse in the presence of multiple user interference. Simulations at a distance of 7m without interference and in the presence of interference have also been performed and the results have been shown in Figures 5.a, 5.b and 5.c. At a distance of 7m the degradation in the performance is more if the number of interferences is increased. At the distance of 7 meters, performance of third derivative of Gaussian pulse is also better than other sub-nanosecond pulses. The results at a distance of 10m and 12m without interference are shown in Figure 6 and in Figure 7 respectively. The result showed that third derivative of Gaussian pulse shows better performance all other pulses.

V. VALIDATION INTO FCC POWER MASK REQUIREMENT

In this section, an analytical approach has been shown for the validation that the third derivative of Gaussian pulse suits the FCC power emission requirement the best among all possible pulse shapes, especially when the wireless channel is impaired with the presence of multiple paths and Multi-user Interference (MUI). According to Part 15 of FCC Regulation on UWB emission limits in the form of a spectral mask for indoor and outdoor systems [12], UWB radios can emit a peak transmit power of -41.3 dBm/MHz in the frequency band from 3.1 GHz to 10.6 GHz. Outside this band, the Power Spectral Density (PSD) must be decreased in order not to interfere with other wireless communication systems operating in that frequency bands. From 0.96 GHz to 1.61 GHz range, the reduction in admissible transmitted power is necessary to protect GPS transmissions. Also, to protect PCS transmission for outdoor systems in the band from 1.99 GHz to 3.1 GHz, the required backoff to be ensured is 20 dB for outdoor systems.

The PSD of the first derivative Gaussian pulse does not meet the FCC power emission requirement regardless of the pulsewidth being used. On the other hand, as indicated in Section 4, it has been found by simulation in our experiment that higher order derivatives of Gaussian pulse have significant E_b/N_o gain for the same BER value over all other pulses used. Therefore, an analytical investigation has been made to research into the PSD of higher order derivatives of Gaussian pulses, more specifically for third derivative of Gaussian pulse. In Figure 8, the normalized PSD has been drawn for first to fifth order derivatives of Gaussian pulse for a chosen value of σ. The value of σ has been calculated according to Bisection method by numerical analysis [14]. The normalization factor is the peak value allowed by the FCC, -41 dBm/MHz. It is clear from the figure that increasing order of derivative increases the center frequency and thus help to suit the FCC power emission regulation, while at the same time reduces the relative bandwidth [14]. Shifting the center (peak) frequency and adjusting the bandwidth so that the FCC requirements are met could be done by modulating the monocycle with a sinusoid by varying the values of σ. But since Impulse radio Ultra Wideband (IR-UWB) systems are carrierless systems, modulation will increase the cost and complexity in design. After an analytical explanation described in Appendix A, it can be concluded that higher order derivatives have a clear impact in fulfilling the FCC PSD mask for UWB transmission and more specifically, third order derivative of Gaussian pulse meets the FCC requirement quite well the 3.1 GHz – 10.6 GHz region while providing a good trade-off between PSD and operational bandwidth. The 3dB bandwidths of higher order Gausian pulses have been calculated and shown in Figure 9 [14]. As order of derivative increases, the relative bandwidth decreases. This point is important for choosing the third order derivative, since its relative bandwidth is much larger than 4th or 5th order derivatives. Also, it has been found from simulation that for the same BER value to be ensured the required E_b/N_o value for the third derivative of the Gaussian pulse is the minimum among all. A more in-depth research is necessary to shape the third derivative of Gaussian pulse so that it fits the FCC PSD requirement more accurately in the 0.96 GHz-1.61 GHz and 1.99 GHz-3.1 GHz ranges. The effectiveness of matched filter in this case can also be investigated.

V. CONCLUSIONS

At present, Ultra Wideband (UWB) radio is an emerging technology especially in short distance indoor communications. In this study, the performance in the form of Bit Error Rate (BER) in MUI environment for Ultra Wideband radio has been described. Stochastic Tapped Delay Line (STDL) model derived basically from Saleh-Valenzuela model and accepted as 'modified S-V model' by IEEE 802.15.3a study group, has been chosen

here to investigate the system performance for various sub-nanosecond pulses and in the presence of multi-user interference. DS-CDMA, a comparatively less complicated and cheaper multiple access technique currently available, is used in the transmitter section. Till date, the most currently adopted and widely accepted pulse shape used for UWB indoor communication is modeled as the second derivative of Gaussian function. [13]. Experiments are still going on so that pulse shapes meet the FCC requirement more accurately. In our experiment, it has been found that third derivative of Gaussian pulse shows the best performance among all pulses used even in the presence of MUI environment. Gausssian pulse and its derivatives have been given more importance because they can be generated at the pulse generator at the easiest way. In our simulation, the best results have been obtained for the third derivative of the Gaussian pulse, where considering the antenna effects is referred as future work of the current research. Through spectral analysis it has also been proved that third derivative of Gaussian pulse fits the FCC power emission mask quite effectively in the 3.1 GHz – 10.6 GHz range where UWB devices are supposed to be used in indoor communications.

REFERENCES

[1] Yomo, H., Popovski, P., Wijting, C., Kovacs, I. Z., Deblauwe, N., Baena, A. F., and Prasad, R. (2001), "Medium Access Techniques in Ultra-Wideband Ad Hoc Networks", paper in the context of the IST-2001-34157 Power aware Communications for Wireless OptiMised personal Area Network (PACWOMAN), the IST program partially funded by the EC. Web: www.imec.be/pacwoman/publications/ WP8-CPK-MAC-UWB-ETAI2003-09-07-2003-V1.0.pdf

[2] D. Barras, F. Ellinger, H. Jäckel, "A comparison between ultra-wideband and narrowband transceivers", TRLabs/IEEE Wireless 2002, Calgary, July 2002

[3] Ramrez-Mireles, F., (2001), "On the Performance of UWB Signals in Gaussian Noise and Dense Multipath," IEEE Transaction on Vehicular Technology, January, Vol. 50, Issue: 1, pp. 244 -249.

[4] Hashemi, H., (1993), "Impulse Response Modeling of Indoor Radio Propagation Channels," IEEE Journal on Selected Areas in Communications, September, Vol. 11, No. 7, pp 967-978.

[5] Win, M. Z. and Scholtz, R. A., (2000), "Ultra wide bandwidth Time Hopping Spread Spectrum Impulse Radio for Wireless Multiple Access Communications," IEEE Transactions on Communications, April, Vol. 48, No. 4, pp 679-691.

[6] Foerster, J. R., (2001), "The Effects of Multipath Interference on the Performance of UWB Systems in an Indoor Wireless Channel," Proceedings of the IEEE Vehicular Technology Conference, VTC Spring 2001, Rhodes, Greece, 6-9 May, Vol. 2, pp. 1176 -1180.

[7] Li, Q. and Rusch, L. A., (2002), "Multiuser Detection for DS-CDMA UWB in the Home Environment," IEEE Journal on selected Areas in Communications, December, Vol. 20, No. 9, pp 1701-1711.

[8] Cassioli, D., Win, M. Z. and Molisch, A. F., (2002), "The Ultra-Wide Bandwidth Indoor Channel: From Statistical Model to Simulations," IEEE Journal on Selected Areas in Communications, August, Vol. 20, No. 6, pp. 1247-1257.

[9] Tesi, R., Hämäläinen, M., Iinatti, J., Oppermann, I. and Hovinen, V. (2004), "On the Multi-User Interference Study for Ultra Wideband Communication Systems in AWGN and Modified Saleh-Valenzuela Channel" in Proceedings of 2004 International Workshop on Ultra Wideband Systems joint with Conference on Ultra Wideband Systems and Technologies, May 18-21, Kyoto, Japan

[10] Conroy, J. T., LoCicero, J. L. and Ucci, D. R., (1999), "Communication Techniques using Monopulse Waveform," Proceedings of the IEEE Military Communications Conference, MILCOM'99 Proceedings, Atlantic city, NJ, USA, 30 October - 3 November, Vol. 2, pp. 1181-1185.

[11] Nee, R. V. and Prasad, R. (2000), "OFDM for Wireless Multimedia Communications", Artech House Boston, USA, ISBN 0-89006-530-6.

[12] Federal Communications Commission, "Revision of Part 15 of the commission's rules regarding ultra-wideband transmission systems, FIRST REPORT AND ORDER," ET Docket 98-153, FCC 02-48, pp. 1–118, February 14, 2002.

[13] Di-Benedetto, M.-G. and Giancola, G. (2004), "Understanding Ultra Wide Band Radio Fundamentals", 1st Edition, 2004, pg. 188, Prentice Hall PTR, New Jersy, USA, ISBN: 0-13-148003-0

[14] Hongsan Sheng, P. Orlik, A. M. Haimovich, L. J. Cimini, Jr. and J. Zhang, "On the spectral and power requirements for Ultra-wideband transmission," in Proceedings of IEEE 2003 International Conference on Communications (ICC), vol. 1, May 2003, Anchorage, AK, pp. 738-742.

APPENDIX: A

Using the expression described in Section 3.A the n-th order derivative of Gausssian pulse can be obtained recursively from

$$\Omega_G^n(t) = -\frac{n-1}{\sigma^2}\Omega^{(n-2)}(t) - \frac{t}{\sigma^2}\Omega^{(n-1)}(t)$$

The Fourier transform of the n-th derivative of Gaussian pulse is

$$\Omega_n(f) = A(j2\pi f)^n e^{-\frac{(2\pi f\sigma)^2}{2}}$$

from where the amplitude spectrum can be considered as

$$|\Omega_n(f)| = A(2\pi f)^n e^{-\frac{(2\pi f\sigma)^2}{2}}$$

The peak emission frequency, f_M can be determined by equating $\frac{d|\Omega_n(f)|}{df}$ to zero. The value of f_M and the corresponding $|\Omega_n(f_M)|$ are found as

$$f_M = \frac{\sqrt{n}}{2\pi\sigma} \quad \text{and} \quad |\Omega_n(f_M)| = A\left(\frac{\sqrt{n}}{\sigma}\right)^n e^{\left(-\frac{n}{2}\right)}$$

The normalized PSD, $|P_n(f)|$ can be defined as

$$|P_n(f)| \equiv \frac{|\Omega_n(f)|^2}{|\Omega_n(f_M)|^2} = \frac{(2\pi f\sigma)^{2n} e^{-(2\pi f\sigma)^2}}{n^n e^{(-n)}}$$

which has a peak value of 1 (0 dB). Considering the n-th derivative of Gaussian pulse as the transmitted pulse of UWB transmission where $A_{\max}$ is the peak power spectral density that has been set as limit by FCC then the PSD of the transmitted signal can be expressed as

$$\left|P_n(f)\right| \equiv A_{\max}\left|P_n(f)\right| = \frac{A_{\max}(2\pi f\sigma)^{2n} e^{\{-(2\pi f\sigma)^2\}}}{n^n e^{(-n)}}$$

It has also been found from the expression of f_M that f_M varies proportionally with $\sqrt{n}$ for a given decaying factor, σ. Gaussian derivatives of higher order are characterized by higher peak frequencies. Thus, differentiation is a way to move energy to higher frequency bands.

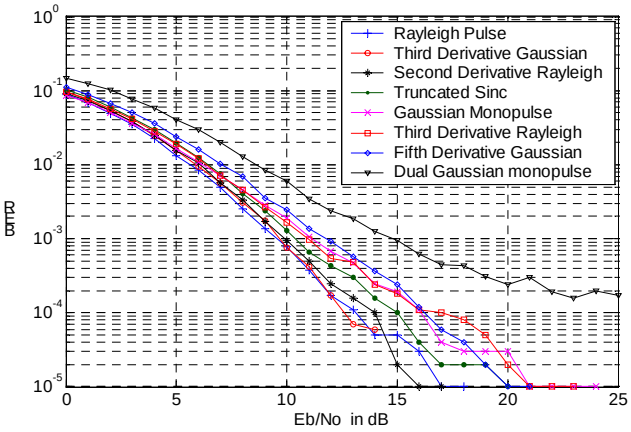

Fig. 3.a: BER performance of different pulses in STDL model of the UWB channel at a distance of 5m in the presence of AWGN with 8 arms

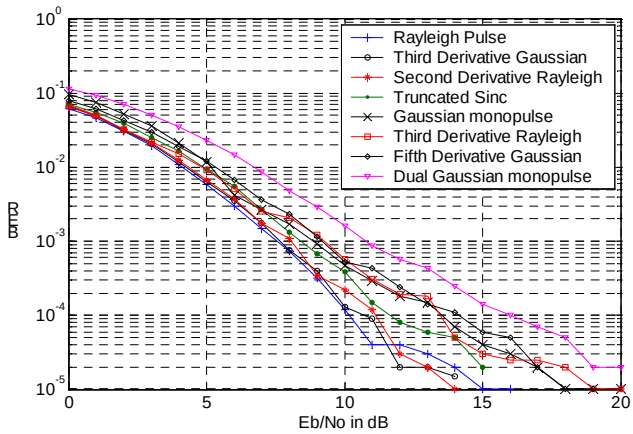

Fig. 3.b: BER performance of different pulses in STDL model of the UWB channel at a distance of 5m in the presence of AWGN with 12 arms

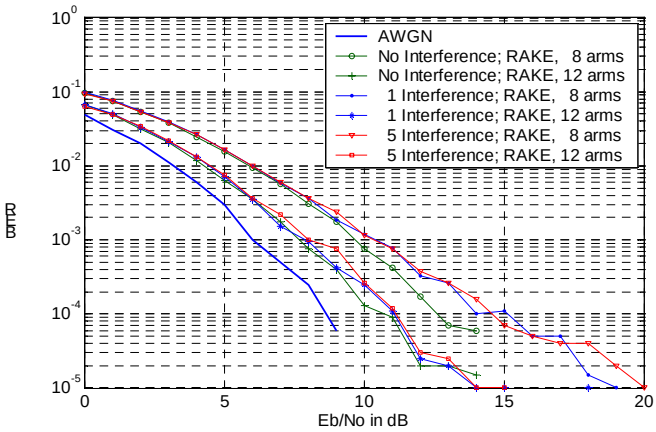

Fig 4.a: Comparison of the performance at a distance of 5m with third derivative Gaussian pulse

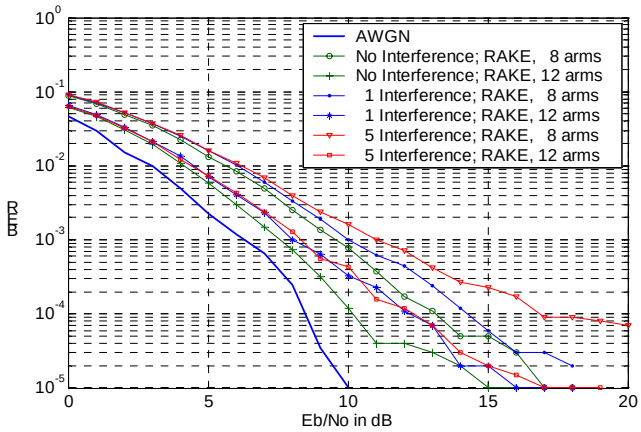

Fig 4.b: Comparison of the performance at a distance of 5m with Rayleigh pulse

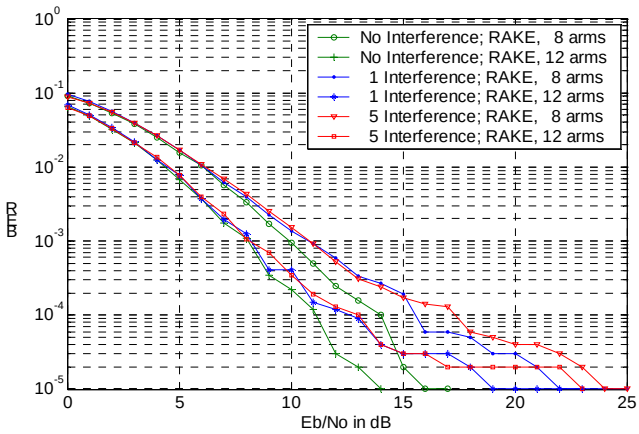

Fig 4.c: Comparison of the performance at a distance of 5m with second derivative Rayleigh pulse

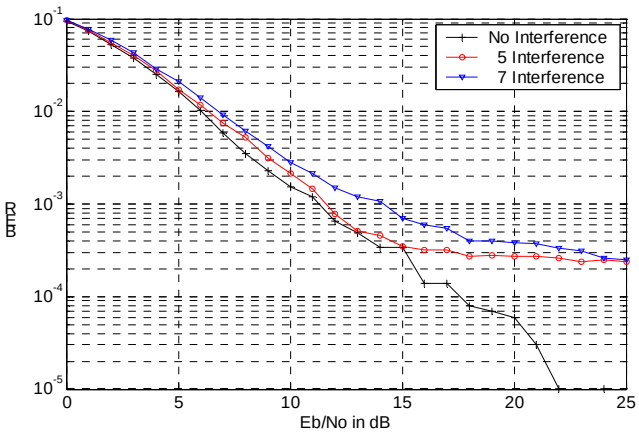

Fig 5.a: Third derivative of Gaussian pulse at a distance of 7m with RAKE 12 arm

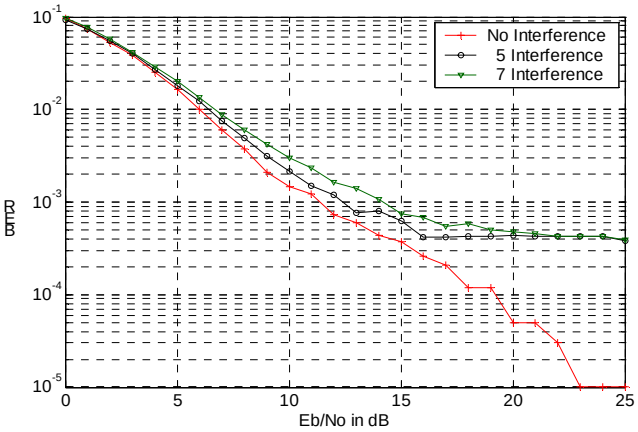

Fig 5.b: Rayleigh pulse at a distance of 7m with RAKE 12 arm

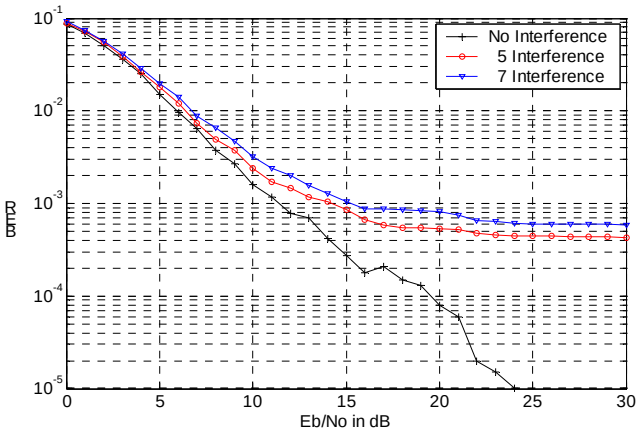

Fig 5.c: Second derivative of Rayleigh pulse at a distance of 7m with RAKE 12 arm

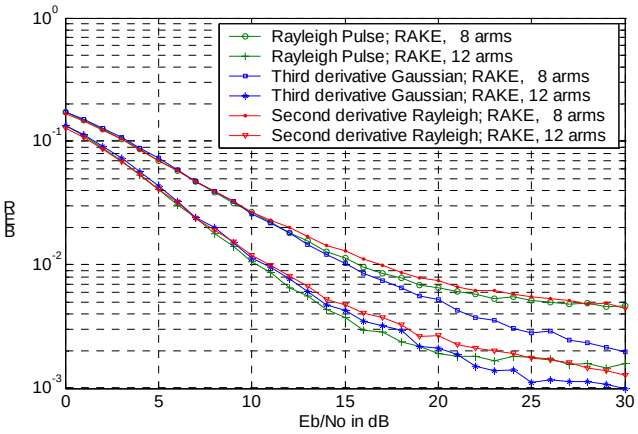

Fig 6: BER Performance of only one user at a distance of 10m

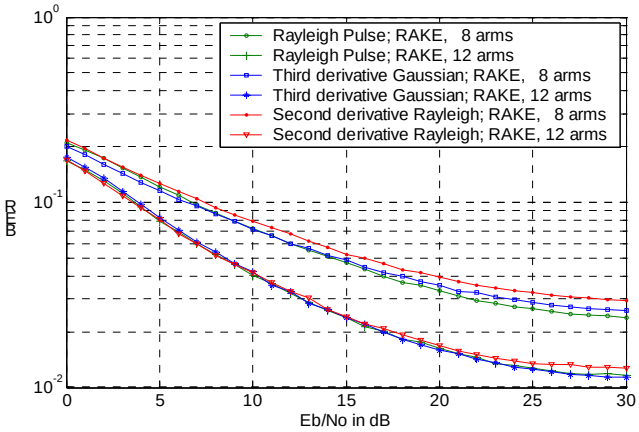

Fig 7: BER Performance of only one user at a distance of 12m

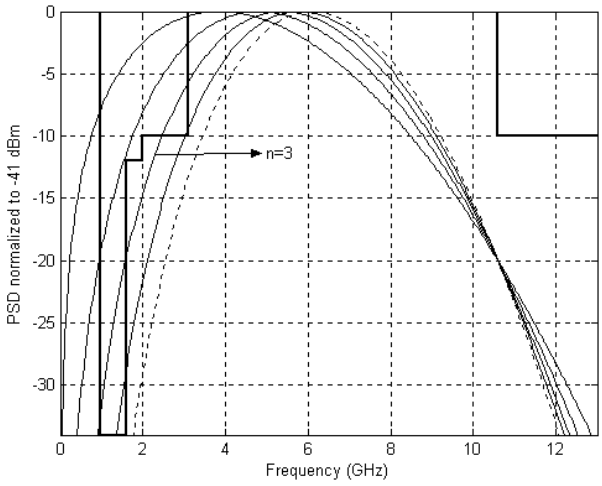

Fig 8: PSD of higher order derivatives of Gaussian pulse for UWB indoor communication

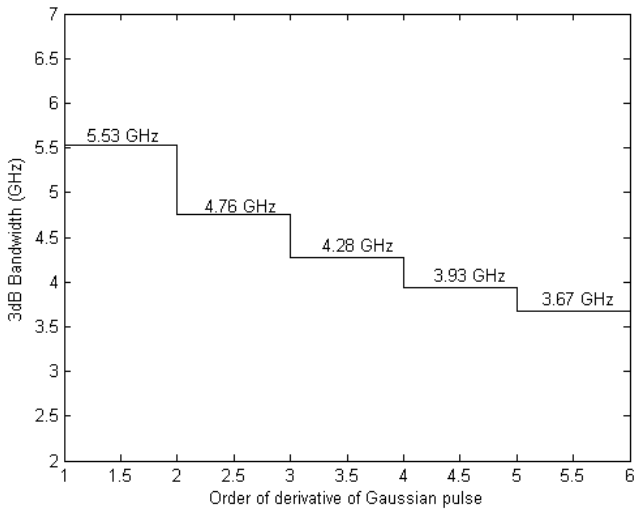

Fig 9: 3dB Bandwidths for higher order derivatives of Gaussian pulse